Food Engineering Progress
Vol. 4, No. 3. pp. 188~192 (2000)

Development of Cold Air Distribution System using Rotating Cone Distributor in Food Storage Facility

Sang-Hoon Ko and Jae-Kun Chun

Department of Food Science and Technology, Seoul National University, Suwon 441-744, Korea

Abstract

To develop cold air distribution system for a cold storage house, a Rotating Cone Air Distributor (RCD, cone-angle 66o) was fabricated and installed in the air-supplying pipe of a pilot scale cylindrical storage house having space of 4.87 m^3. The design factors and mechanical operation mechanism of the RCD was investigated for the focusing supply of cold air. The flow rate and direction of cold air flow was controlled by regulating alignment of the cone of the RCD against the inlet air stream, and the alignment was controlled by a stepping motor manipulated with a microcontroller. The relationship between the flow rate of the cold air and the cone angle was established on the basis of aperture area and shape. The automatic operation program for the RCD control was developed and the performance test of the air distribution system was conducted in a field condition with successful controls of airflow rate and direction. The RCD system was proved to be effective for the intensified cold air-supply to a specific warmer zone in the storage house.

Key words: cold food storage, air distribution, rotating cone air-distributor

Introduction

Cold storage method is widely used as one of the important storage technology because microbial and biochemical activities in food are suppressed under cold storage condition (Lawrence *et al.*, 1986). The severe damages in food quality frequently give rise to the increased spoilage at warmer zone and the physiological cold injury at colder zone in the same storage room. Therefore, it is important to resolve the thermal localization phenomena and to prevent the localization throughout storage period for the quality preservation (Fuchigami *et al.*, 1995; Hanenian *et al.*, 1989; Ha *et al.*, 1985, Heldman, 1982).

The control factors of food storage system are the cooling capacity and cooling rate of the storage facility, and thermal properties of food under storage. They are all temperature dependents. Among the factors, cooling rate of the storage room is the most important in bringing down the food temperature (Ashrae, 1977; Snow, 1950; Sastry, 1984).

The cause of the thermal localization comes from two reasons: cold air supplying system and thermal state of food commodity (Cleland *et al.*, 1979; Lightfoot *et al.*, 1965; Hung and Thompson, 1983). In these aspects, it is required to design a more flexible air distribution system to release thermal problems in the storage room.

The objective of this study was to develop the cold air distribution system with a rotating cone distributor to improve cold air distribution in the cylindrical floated rotating storage facility.

Corresponding author: Jae-Kun Chun, Department of Food Science and Technology, School of Agricultural Biotechnology, Seoul National University, Suwon 441-744, Korea

Materials and Methods

Food storage facility

A cylindrical rotating storage facility (4.87 m^3 volume, 2 m diameter, 1.55 m height) developed by Kim and Chun (1998) was used with a major modification in air supplying system. The modified storage facility consisted of a cylindrical floated rotating wall, a gas-tight door, an upper duct and a bottom duct. Cooling system of the storage facility was composed of a compressor (1HP, F22 refrigerant, Tecumseh, USA), a condenser

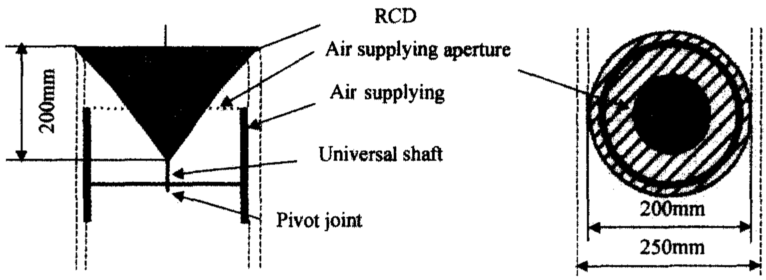

(a) Side view

(b) Top view

(Cross hatched circular is the baffle disk of RCD)

Fig. 1. The structure of rotating cone distributor (RCD) (cross hatched circular is the baffle disk of RCD).

(6.2 m^2, heat transfer area; 1.55 kJ/h, capacity; Chun-gang Co., Korea), an evaporator and a defrost heater (1.8 kW, Korea). Control system for the food storage facility was constructed with single-chip food process controller (SFPC) developed by Kwon and Chun (1995), magnetic contacts, and overload protective relays.

Rotating cone distributor (RCD) system

An acrylic plate (thickness, 5 mm) was used to fabricate a rotating cone distributor (RCD). The RCD system was composed of a RCD, a connecting rod (stainless steel, diameter 5 mm, length 40 mm), a stepping motor (2-phase hybrid motor, 1.8°/step, 12V DC, 0.4A, KH42J M2-505) and a stepping motor driver (24V DC, SERVEX-FSD2U2P12, Japanservo Co., Japan).

Airflow control system

An airflow control system was built to control airflow rate and direction by regulating the alignment of the RCD system. Airflow rate was controlled by changing the size of aperture area forming between the RCD and air supplying duct by adjusting the height of connecting rod of the RCD system (See Fig. 2). Airflow direction was controlled by changing the alignment of the RCD.

Results and Discussion

Design and fabrication of the Rotting Cone Distributor

The RCD was designed to change the cold airflow direction to various locations in the storage room with varying the angle of a triangular cone alignment against t

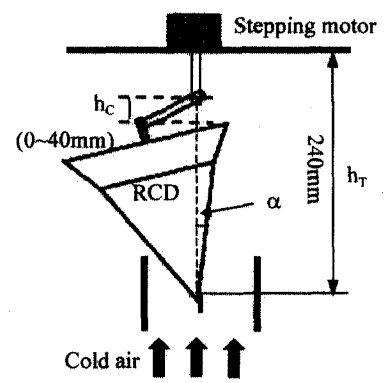

Fig. 2. The control mechanism of air supplying aperture.

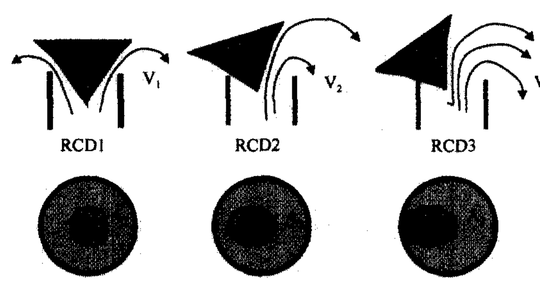

Fig. 3. The air-supplying apertures formed at various inclined angles of the RCD.

he inlet air stream as shown in Fig. 2. The circular disc of the cone acted as an air guide baffle to regulate the air supplying aperture to affect the direction of cold air.

A universal connecting shaft of the RCD was seated at the pivot joint in the center of the air supplying duct and the upper part of the shaft was connected to the stepping motor (Fig. 1 and 2). Due to the concentricity between the shaft of stepping motor and the pivot joint of air supplying duct, the RCD was able to incline with the change of the net height of the connecting rod (Fig. 2).

Airflow rate control mechanism

The air supplying aperture was varied in respect to the inclined angle of the RCD as shown in Fig. 2. When the alignment of the RCD stood at upright position without inclining (maximum connecting rod height), the shape of air supplying aperture was formed like a doughnut as appeared in Fig. 3. The larger inclined angle was, the greater eccentricity of the aperture was. The eccentricity of the aperture is dependent on the ratio of effective height of the connecting rod (h_C) to total RCD height (h_T). The eccentricity (ε) of the aperture can be expressed as follows:

$$\varepsilon = f\left(\frac{h_C}{h_T}\right) = k_\varepsilon h_C \quad (1)$$

where k_ε is an eccentric coefficient. The eccentricity was controlled by h_C. as shown in Fig. 2. The relationships between the inclined angle (α) of the RCD and the eccentricity of air supplying aperture is shown in Fig. 3.

Control mechanism of airflow direction

Airflow direction was controlled by the angle of the RCD as illustrated in Fig. 4. Due to the eccentric nature of the aperture, the airflow direction was varied by the angle of gyratorial RCD. Accordingly, the airflow direction marked with arrow in Fig. 4 was determined by the angle of the RCD.

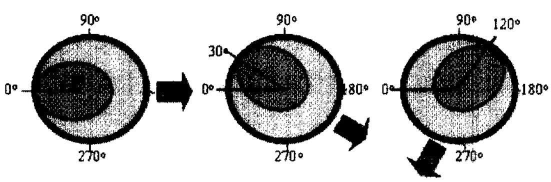

Fig. 4. The relationship between the angle of RCD and air flow direction at the alignment RCD (the solid arrow indicates the direction of airflow with angle specified).

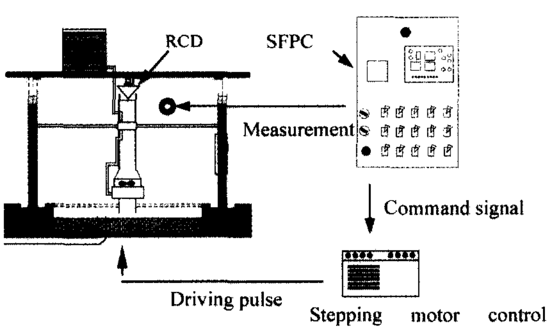

Fig. 5. The food storage facility constructed with the RCD control.

Construction of the RCD control system

To embody the airflow control mechanism, the RCD control system was installed to the storage facility as shown in Fig. 5. The SFPC measured environmental values from temperature sensors inside the storage room and manipulated actuators such as stepping motor, compressor and fan. The RCD was controlled with feedback method by the SFPC using a stepping motor control module. The high-low square pulses were generated and transmitted to output port of the SFPC. The stepping

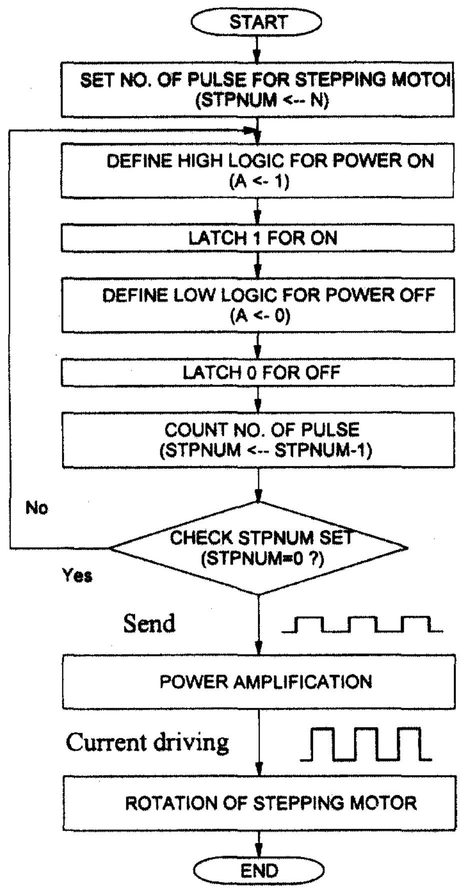

Fig. 6. The pulse generating program for the RCD control.

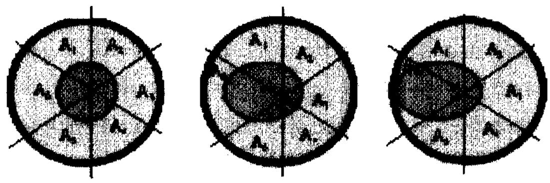

(a) RCD1 (b) RCD2 (c) RCD3

Fig. 7. The RCD alignments and cross section areas of aperture. RCD1, non-inclined alignment; RCD2, half-inclined align-ment; RCD3, full-inclined alignment; Aj, segmental aperture areas of each RCD alignment.

motor control module converted the pulses to the equivalent driving pulses to rotate the stepping motor. The pulse generation program for the RCD control is illustrated in Figure 6. The stepping motor had 1.8° angle resolution and 200 pulses were required for one revolution (360°) of the RCD.

Relationship between RCD alignment and airflow air distribution

Fig. 7 shows the air stream patterns at various angles of the RCD. Because of the complexity of the aerodynamic property around the RCD, the aperture was divided into six segments (A1, A2, A3, A4, A5 and A6) in respect to three alignments: RCD1, RCD2 and RCD3.

To estimate the airflow rate through the aperture of the RCD, the relationship between the alignment of the RCD and the effective aperture (Fig. 7) was analyzed.

An airflow rate is affected by the RCD alignment. If the mass flow rate of cold air is constant, the airflow rate at cross-sectional aperture can be estimated. For each RCD aperture, the continuity equation of airflow is expressed as follows:

$$v_0 A_0 = \sum_{j=1}^{6} v_j A_j \qquad (2)$$

where v_0, A_0, v_j and A_j are inlet air velocity, cross sectional area of the air supplying duct, segmental air velocity of aperture and segmental areas of aperture, respectively.

Assuming the friction energy at the RCD negligible, six segmental air velocities (v_j) of each RCD aperture will be proportional to the sectional area of each aperture

Table 1. The airflow rates at various aperture sections in respect to the RCD alignments

RCD alignments with air velocity	Section of aperture	Area (cm^2)	Airflow rate ($kg/s \times 10^{-2}$)	Air distribution rate (%)
RCD1 υ_m=4.17 m/s	A_1	44.0	2.29	16.67
	A_2	44.0	2.29	16.67
	A_3	44.0	2.29	16.67
	A_4	44.0	2.29	16.67
	A_5	44.0	2.29	16.67
	A_6	44.0	2.29	16.67
	A_{total}	264.0	13.74	100
RCD2 υ_m=4.29 m/s	A_1	42.6	2.28	16.60
	A_2	47.9	2.56	18.66
	A_3	48.9	2.61	19.05
	A_4	47.9	2.56	18.66
	A_5	42.6	2.28	16.60
	A_6	26.6	1.42	10.37
	A_{total}	256.5	13.71	100
RCD3 υ_m=4.33 m/s	A_1	42.3	2.28	16.65
	A_2	52.9	2.85	20.82
	A_3	52.9	2.85	20.82
	A_4	52.9	2.85	20.82
	A_5	42.3	2.28	16.65
	A_6	10.6	0.57	4.17
	A_{total}	253.9	13.68	100

as described in Equation (3).

$$v_j = v_m \tag{3}$$

$$v_0 A_0 = \sum_{j=1}^{6} v_j A_j = \sum_{j=1}^{6} v_m A_j = v_m \sum_{j=1}^{6} A_j = v_j A \tag{4}$$

where v_m is the mean air velocity.

Therefore, the air velocity and air supply mass at each RCD aperture can be estimated by Equation (5) and (6), respectively.

$$v_m = n_0 \frac{A_0}{A} \tag{5}$$

$$W = n_m \rho A \tag{6}$$

where ρ is air density and W is air mass.

Calculation of the airflow rates at various sections of air supplying aperture

The airflow rates at the aperture segments were calculated using Equation (5) and (6), respectively. At RCD1 alignment, air velocity was 4.17 m/s with uniform airflow distribution all over the cross-sections. And air velocities were 4.29 m/s at RCD2 and 4.33 m/s at RCD3. As increasing angle of the RCD, airflow rates were increased. The airflow rates at various segments of the aperture are shown in Table 1.

For the effective distribution of cold air in the food storage room, a new air distributor - rotating cone distributor (RCD) system - was developed. The RCD system performed successfully cold air distribution by the RCD control system in the food storage facility. The intensified cold air supply to a specific warmer zone was also achieved by the RCD system.

In our system, cold air was circulated upward from bottom with the propeller fan. Correspondingly, vortex airflow was developed and circulated along the inner wall of the cylindrical storage room. According to the tangential flow pattern, the target position for focusing cooling was shifted around 90~120°. The directional angle ship is expected to solve with the software program. Through this field scale application, a flexible cold air supply both in the cooling rate and in direction was successfully demonstrated.

References

Cleland, A.C. and R.L. Earle. 1979. A comparison of methods for predicting the freezing times of cylindrical and spherical foodstuffs. *J. Food Sci.* **44**: 958-970

Fuchigami, M., N. Hyakumoto and K. Miyazaki 1995. Texture and pectic composition differences in raw, cooked and frozen-thawed Chinese cabbages due to leaf position. *J. Food Sci.* **60**(1): 153-156

Ha, J.S., W.N. Kim, K.K. Kim and C.A. Oh. 1985. Study on the optimum control of refrigerator with on-off control system. *J. Korea Soc. Marine Engineers* **9**(4): 317-327

Hanenian, R., G.S. Mittal, and W.R. Usborne. 1989. Effects of pre-chilling, freezing rate, and storage time on beef patty quality. *J. Food Sci.* **54**(2): 532-535

Heldman, D.R. 1982. Food properties during freezing. *Food Technology* **36**(2): 92-96

Hung, Y.C. and D.R. Thompson. 1983. Freezing time predictions for slab shape foodstuffs by an improved analytical method. *J. Food Sci.* **48**: 555-560

Lawrence, R., F. Consolacion and P. Jelen. 1986. Formation of structured protein foods by freeze texturization. *Food Technology* **40**(4): 77-90

Lighfoot, B.N., C. Massot and F. Irani, 1965. Approximate estimation of heat and mass transfer coefficients. *AICHE Chemical Engineering Symposium Series* **61**(58): 25

Kim, H.Y. and J.K. Chun. 1998. Gas tight rotating wall system by hydraulic lock mechanism. MS thesis, Seoul National University

Kwon, S.H. and J.K. Chun. 1995. Design of multi-purpose agricultural controller and development of its operation program. MS thesis, Seoul National University

Sastry, S.K. 1984. Freezing time prediction: An enthalpy-based approach. *J. Food Sci.* **49**: 1121-1127

Snow, J.M. 1950. Proteins in fish muscle. Denaturation of myosin by freezing. *J. Fisheries Res. Board Can.* 599